ACS Sustainable Chemistry & Engineering

Research Article

pubs.acs.org/journal/ascecg

Using Cellulose Nanocrystals as a Sustainable Additive to Enhance Hydrophilicity, Mechanical and Thermal Properties of Poly(vinylidene fluoride)/Poly(methyl methacrylate) Blend

Zhen Zhang,[†] Qinglin Wu,*[,†] Kunlin Song,[†] Suxia Ren,[‡] Tingzhou Lei,*[,‡] and Quanguo Zhang[§]

[†]School of Renewable Natural Resources, Louisiana State University, Baton Rouge, Louisiana 70803, United States

[‡]Key Biomass Energy Laboratory of Henan Province, Zhengzhou, 450008 Henan, China

[§]Collaborative Innovation Center of Biomass Energy of Henan Province, College of Mechanical and Electrical Engineering, Henan Agricultural University, Zhengzhou, 450002 Henan, China

Supporting Information

ABSTRACT: The aim of this study is to use cellulose nanocrystals (CNCs) as a sustainable additive for improving hydrophilicity, mechanical and thermal properties of poly(vinylidene fluoride) (PVDF)/poly(methyl methacrylate) (PMMA) blends. A casting-evaporation method was used to prepare the nanocomposites, and their surface wettability, mechanical, thermal and morphological properties were characterized. With the addition of only 3 wt% CNCs, tensile strength, tensile modulus, dynamic storage modulus at 45 °C, and onset thermal decomposition temperature of the ternary composite exhibited 32%, 70%, 36% and 4.0 °C increase, respectively, while the static water angle decreased by 6°. As the CNC content increased to 6 wt %, further improvement was observed in all above properties except tensile strength. The observed performance enhancement is attributed to a considerably increased crystallinity of PVDF (e.g., from 28.5% for the binary blend to 43.3% for ternary composite at the 3 wt % CNC level). Our present work demonstrates the importance of using sustainable CNCs to achieve synergetic improvement in physical and mechanical performance of PVDF/PMMA blend, suggesting a facile way to prepare nanocomposites for potential membrane-based separation applications.

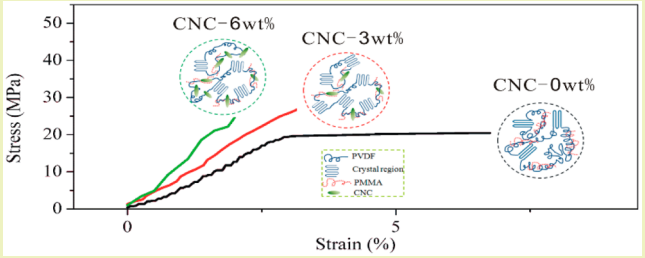

KEYWORDS: *Cellulose nanocrystals, poly(vinylidene fluoride), sustainability, reinforcement, hydrophilic modification*

INTRODUCTION

Poly(vinylidene fluoride) (PVDF), as a semicrystalline polymer derived from petroleum resources, has been widely used in membrane-based separating operations because of its outstanding properties including thermal, chemical, oxidation resistance and exceptional hydrolytic stability.[1−3] However, the PVDF materials are hydrophobic, which is a notable drawback, especially when they are used for ultrafiltration operations for aqueous solutions. In this circumstance, PVDF is susceptible for contamination by proteins and some other impurities in water treatment, due to its hydrophobic nature. This contamination can cause a sharp drop in the water flux of the membrane[3,4] and therefore leads to reduced productivity and increased energy consumption. To overcome this drawback, blending PVDF with another hydrophilic polymer has been practiced as an inexpensive technique. Several pairs of PVDF-based blends, including PVDF/poly(methyl methacrylate) (PMMA), PVDF/poly(vinylpyrrolidone), PVDF/sulfonated polystyrene and PVDF/poly(vinyl acetate) have been reported.[5] However, there are three limitations of this strategy. First and foremost, the efficiency of hydrophilic modification is low. For instance, even with the addition of 50 wt % PMMA[1] and poly(styrene-*co*-acrylonitrile) (SAN),[6] the decrease in static water contact angle was 11° and 6°, respectively, which are of low modifying efficiency. Second, the addition of another hydrophilic polymer component failed to effectively enhance the mechanical properties of PVDF membrane.[7−9] Third, most of the aforementioned hydrophilic polymers and PVDF come from petroleum source, and the prepared polymer blends are not sustainable. Thus, it is highly attractive to use a renewable natural resource to effectively enhance both hydrophilicity and strength of PVDF.

Cellulose nanocrystals (CNCs) are of sustainable nature, coming from the most abundant resources such as wood, plants, bacteria and truncate.[10−13] Through acid and/or enzymatic hydrolysis of cellulosic materials, CNCs with highly crystalline rod-like nanostructures are obtained.[10] CNCs are water-dispersible renewable materials and have high hydrophilicity. Previously, cellulose acetate (CA), a derivative of cellulose (of the same origin as CNCs), has been successfully used to modify the surface wettability of PVDF.[14] For mechanical reinforcement, CNCs have been considered as

Received: August 26, 2014
Revised: January 24, 2015
Published: January 29, 2015

DOI: 10.1021/sc500792c
ACS Sustainable Chem. Eng. 2015, 3, 574−582

one of the ideal reinforcing fillers due to their high tensile strength (~7 GPa) and Young's modulus (~130 GPa).[15] Previous studies reported the reinforcing effect of CNCs on several kinds of polymers such as poly(ethylene oxide),[15] PMMA,[16] poly(propylene carbonate),[17] poly(L-lactic acid)[18] and polyurethane.[19] In addition to the stiff nature of CNCs, for semicrystalline polymers like PVDF, the presence of nanofillers might influence the crystal structure of polymeric matrix (e.g., crystallinity),[17] and thereby improve the mechanical strength. Our previous study[20] also shows that CNCs can favor the nucleation and crystallization of PVDF/PMMA blend. Considering both rigid nature of CNCs and their influence in the crystal structure of PVDF/PMMA blend, it is hypothesized that CNCs can be used to effectively improve the mechanical properties of the composite.[21]

In this work, both 30 wt % PMMA and CNCs were used to modify PVDF via a solution-casting technique. PMMA was used due to its good compatibility with PVDF,[1] which is a premise of good properties of blend, and lower material cost compared with PVDF. However, only limited improvement in hydrophilicity of PVDF was achieved with the use of 30 wt % PMMA. On the other hand, the addition of CNCs contributed to a considerable improvement in hydrophilicity, leading improved sustainability with less nonsustainable hydrophilic polymers needed to achieve the same level of hydrophilicity. To the best of our knowledge, the effect of CNCs on the mechanical, hydrophilic and mechanical properties of PVDF/PMMA blend has not been reported. We herein exploit CNCs as a sustainable additive to modify PVDF/PMMA (70/30) blends via a casting-evaporation method. For a comparison purpose, the tensile properties and water contact angle results of PVDF, PMMA, PVDF/PMMA (50/50) and PVDF/SAN (50/50) were also reported. The specific mechanisms for the improved mechanical, thermal properties and hydrophilicity were fully elucidated.

EXPERIMENTAL SECTION

Materials and Sample Preparation. PVDF (Kynar K-761, M_w = 441 000, Elf Atochem of North America Inc.), PMMA (GF1000, Kurkaray) and SAN (PN139H, Zhenjiang Qimei Chemical Co., Ltd., China) were used in this study. The CNCs were of cotton origin, and the specific preparation procedure was described in our previous paper.[22] In general, CNCs were prepared via the combination of acid hydrolysis using 64% H_2SO_4, high-pressure homogenization and freeze-dried processes. The average length and diameter of CNCs was 159 ± 57 and 15.0 ± 4.5 nm, respectively.[22] The solution blending technique was utilized and DMF worked as the solvent. The concentration of polymer blend was fixed at 10 wt %, whereas the concentration of CNCs in relation to the polymer blend was set at 0, 3 and 6 wt %, respectively. The specific formulations were PVDF, PMMA, PVDF/PMMA (70/30) blend, PVDF/PMMA (50/50) blend, PVDF/SAN (50/50) blend, PVDF/PMMA (70/30) composite with 3 wt % CNCs and PVDF/PMMA (70/30) composite with 6 wt % CNCs, which were designated as P, M, PM3, PM5, PS5, PM3C3 and PM3C6, respectively.

For the preparation of polymer and polymer blends, the polymer was first dissolved in DMF. In the preparation of nanocomposites, freeze-dried CNCs were dispersed in DMF and were ultrasonicated for several hours to get a homogeneous suspension. The CNC suspensions were then mixed with PVDF/PMMA (70/30) solutions with a target composition under the condition of vigorous stirring overnight. The suspension was casted in a glass Petri dish, which was kept at 50 °C in a vacuum oven for 48 h. Finally, the thin film with a thickness of about 80 um was obtained and peeled off from the dish. To remove any residual DMF in the manufactured films, the films were immersed in fresh ethanol at room temperature for 12 h. Then, the ethanol was replaced with the fresh ethanol. Such a step was repeated for 9 times. After the extraction process, the film was dried in a vacuum oven at 25 °C for 12 h. After that, samples without DMF residual were obtained. Characterization that was used to determine whether the extraction method completely eliminated the DMF residue from the film is presented the Supporting Information (Figure S1).

Characterizations. Tensile properties of the film were investigated using an AR2000EX rheometer (TA Instruments-Waters LLC, New Castle, DE) configured to a static tensile loading mode with a solid fixture. The load cell capacity of the rheometer was 50 N. The dimension of each rectangle sample, obtained by cutting from film samples, was 15 mm (length), 3 mm (width) and 0.1 mm (average thickness). The gauge length was set as 10 mm and the testing speed was 1.2 mm/min. The principle of the tensile test using a rheometer can be found in our previous paper.[15] Tensile strength, tensile modulus and elongation at the break were calculated from the machine-recorded force and displacement.

Surface wettability tests were carried out using a model FTA 200 contact angle analyzer (First Ångstorms Inc., Falls Church, VA) at room temperature with a static test method. Droplets of deionized water were delivered onto the surface of each specimen. Three water contact angle measurements on each sample surface were taken with an accuracy of ±2°.

Thermal stability of neat CNCs, PVDF/PMMA (70/30) blend and the composites was measured using a TA thermogravimetric (TG) analyzer (Q-50, TA Instruments-Waters LLC, New Castle, DE). Each sample of about 4 mg was heated from room temperature to 600 °C at a heating rate of 10 °C/min. Nitrogen atmosphere was introduced with a nitrogen gas flow at a rate of 60 mL/min.

Dynamic mechanical analysis (DMA) tests were carried out with a dynamic mechanical analyzer (Q800, TA Instruments-Waters LLC, New Castle, DE). Each sample was scanned from 40 to 180 °C under tension mode and a heating rate of 2 °C/min. The constant frequency was 3 Hz and the strain amplitude was 0.1%. The dimension of each sample is 20 mm (length), 5 mm (width) and 80 um (average thickness).

A Q200 differential scanning calorimeter (TA Instruments-Waters LLC, New Castle, DE) was used to investigate the melting and crystallization behaviors of the blend and composites. Each sample (about 3 mg) was first scanned from room temperature to 200 °C at a rate of 40 °C/min and was kept for 5 min in order to eliminate any thermal history. And then the sample was cooled to 40 °C at a rate of 5 °C/min and maintained for 5 min to observe the crystallization behavior. To observe the melting behavior of samples without previous thermal history, a second heating scan was recorded from 40 to 200 °C at a rate of 10 °C/min. Nitrogen purge gas with a flux rate of 40 mL/min was introduced.

The crystallinity (X_c) of PVDF was calculated as follows

$$X_c = \frac{\Delta H_m/\phi}{\Delta H_m^*} \times 100\% \quad (1)$$

where ΔH_m is the melting enthalpy measured from the differential scanning calorimetry (DSC) curves, $\Delta H_m^*$is the melting enthalpy when crystallinity of the polymer is 100% and φ is the weight fraction of PVDF in the blend and composites. The ΔH_m^* value of PVDF reported in the literature is 104.5 J/g.[23] The crystallization half time ($t_{1/2}$), which is the time when the relative degree of crystallization (X_t) is 0.5, was also used to characterize the crystallization process. X_t was calculated as follows

$$X_t = \left[\int_{T_0}^{T} (dH_c/dT) \times dT\right] / \left[\int_{T_0}^{T_\infty} (dH_c/dT) \times dT\right] \quad (2)$$

where T_0, T_∞ and T are the onset crystallization temperature, end crystallization temperature and crystallization temperature at time t, respectively, and H_c is the enthalpy of crystallization. Crystallization time was calculated by the following equation, in which Φ is the cooling rate:

DOI: 10.1021/sc500792c
ACS Sustainable Chem. Eng. 2015, 3, 574−582

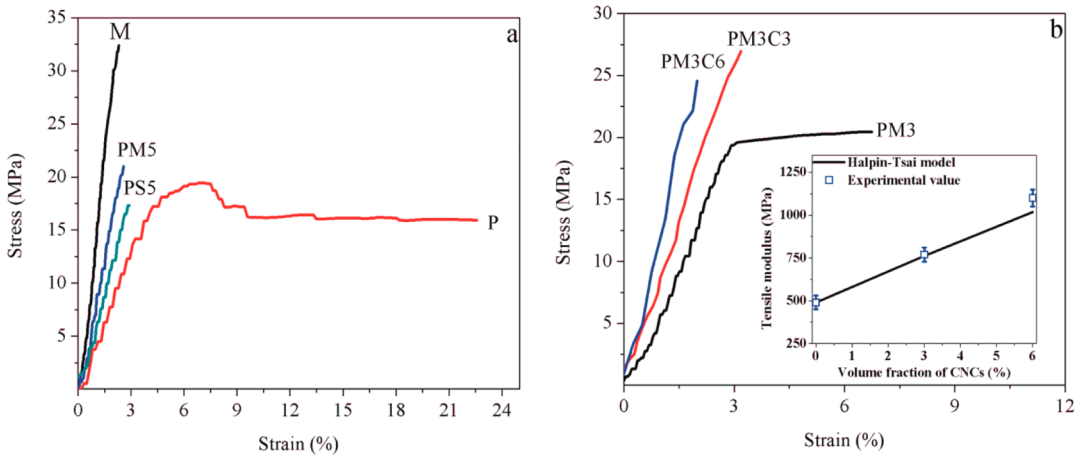

Figure 1. Typical stress–strain curves of different materials: (a) pure polymers and polymer blends; (b) PVDF/PMMA (70/30) blend and its composites.

$$t = |t_0 - t|/\Phi \quad (3)$$

Dynamic rheology used to monitor storage modulus of film was performed using two parallel plates with a time sweep measurement using the AR2000EX rheometer (TA Instruments-Waters LLC, New Castle, DE). Each film was heated at 200 °C and was held for 5 min in order to completely melt polymers in the sample and to remove any residual crystallinity. Then, the samples were cooled to 135 or 145 °C at a cooling rate of 50 °C/min. Once the predetermined crystallization temperature (135 or 145 °C) was reached, a frequency of 1 s^{-1} and a strain of 1% were immediately applied. Measurements were conducted until the storage modulus leveled off.

To further investigate the phase morphology, the cryo-fractured surface of neat PVDF/PMMA blend and the ternary composites were disclosed using a field emission scanning electron microcopy (FEI QuantaTM 3D FEG Dual Beam SEM/FIB, Hillsboro, Oregon, USA). The cryo-fractured surfaces were coated with a thin layer of platinum before viewing. The accelerated voltage was 5 kV. No staining or chemical treatments of the samples were used for this measurement.

Fourier transform infrared spectroscopy (FTIR) measurements of the blend and its composites were performed on a Bruker FTIR analyzer (Tensor-27, Bruker Optics, Billerica, MA) with an attenuated total reflectance (ATR) mode. A transmission mode combined with 32 scans and a spectral range of 4000–600 cm^{-1} was used.

RESULTS AND DISCUSSION

Mechanical Properties. Figure 1a shows typical stress–strain curves of pure polymers and polymer blends. Pure PVDF exhibited a well-defined yielding behavior (curve P). For PMMA (curve M), PVDF/PMMA (50/50) blend (curve PM5) and PVDF/SAN (50/50) blend (curve PS5), no plastic yielding behavior was observed and the samples were fractured before the strain reached the yielding region. The mechanical parameters derived from the stress–strain curves are summarized in Table 1. As shown, pure PMMA had higher values of tensile strength and modulus than those of pure PVDF. The use of PMMA helped improve the tensile modulus and slightly enhance the tensile strength as well. However, the addition of SAN improved tensile modulus somewhat, but lowered the strength.

After CNCs were introduced into the PVDF/PMMA (70/30) matrix, a considerable reinforcement was observed. Similar to the behavior of PVDF, the PVDF/PMMA (70/30) blend also exhibited a yielding behavior (Figure 1b). Limited increases in both tensile strength and modulus were seen for blend in comparison with pure PVDF (Table 1). However, with

Table 1. Tensile Properties of Different Materials Made from This Work

sample[a]	tensile strength (MPa)	tensile modulus (MPa)	elongation at break (%)
P	18.8 ± 1.2	452 ± 36	23 ± 4
M	32.4 ± 1.0	1140 ± 60	2 ± 1
PM3	20.4 ± 1.1	520 ± 42	7 ± 2
PMC3	27.0 ± 2.0	882 ± 38	3 ± 1
PMC6	24.6 ± 1.8	1100 ± 40	2 ± 1
PM5	21.3 ± 1.0	745 ± 48	3 ± 1
PS5	17.3 ± 1.3	494 ± 32	3 ± 1

[a]P-PVDF; M-PMMA; PM3-P/M (70/30); PM3C3-P/M (70/30) with 3 wt % CNCs; PMC6-P/M (70/30) with 6 wt % CNCs; PM5-P/M (50/50); PS5-P/SAN (50/50).

increase of CNCs from 0 to 3 wt % in the blend, the tensile strength increased from 20.4 to 27.6 MPa, and tensile modulus from 520 to 882 MPa, which corresponded to 35% and 70% improvement, respectively. Further addition of CNCs contributed to a continuous increase in tensile modulus (112% increase compared with that of the pure blend), but a slight decrease in tensile strength was observed. Similar trends in tensile strength for CNC-reinforced composites were also reported elsewhere.[18]

For ductility, incorporation of both polymers (i.e., PMMA and SAN) and CNCs caused the decline in the elongation at break. This was thought to be due to the low ductile nature of neat polymer, and to the existence of nanoparticles, which can lead to stress concentrations under tensile loadings.[24,25] As a result, the composites were fractured at lower strains for composites with increased CNCs content. Since both polymers and CNCs decreased the elongation at break and CNCs exhibited a more effective reinforcement, CNCs had an obvious advantage for enhancing the mechanical properties.

To investigate the reinforcing potential of CNCs within PVDF/PMMA matrix, a common model developed by Halpin–Tsai was used to compare with the experimental data. According to the Halpin–Tsai model, theoretical modulus of composites can be calculated with the following equations:[26]

$$E = E_m(1 + \xi\eta\varphi)(1 - \eta\varphi) \quad (4)$$

$$\eta = (E_r/E_m - 1)(E_r/E_m + \xi) \quad (5)$$

DOI: 10.1021/sc500792c
ACS Sustainable Chem. Eng. 2015, 3, 574–582

$$\xi = 2xl/d \quad (6)$$

where E is the composite modulus (MPa), E_m is the modulus of the matrix (MPa), E_r is the modulus of the filler (MPa) and ϕ is the volume fraction (%). ξ is a shape parameter related to the aspect ratio of filler. ξ can be calculated using the length (l) and diameter (d) of CNCs. For relatively short fibers like CNCs, eq 6 can be simplified as $\xi = 2l/d$.[27] The following values for the matrix and the CNCs were used for the theoretical calculations: E_m = 520 MPa based on tensile results, E_r = 145 000 MPa,[29] ρ_m = 1.60 g/cm^3 and ρ_r = 1.59 g/cm.[3,27] The length of the CNCs was 159 nm and the diameter was 15 nm according to the transmission electron microscopy (TEM) results from our previous study.[24] The volume fractions of CNCs were calculated using the following equation:

$$\varphi = (w_r/\rho_r)/((w_r/\rho_r) + (1 - w_r)/\rho_m) \quad (7)$$

The comparison between the experimental results and the predicted data from the Halpin−Tsai model is shown in the inset of Figure 1b. It is known that the Halpin−Tsai model is based on composite systems where the fillers are aligned in the longitudinal direction, and have a perfect interfacial adhesion to the matrix and a good dispersion within the matrix.[26] Here, the experimental values of tensile modulus well followed the values predicted by the Halpin−Tsai model, indicating a possible good dispersion of CNCs within the polymeric matrix.

The storage modulus of the blends and composites further verified the reinforcing effect of CNCs. As shown in Figure 2,

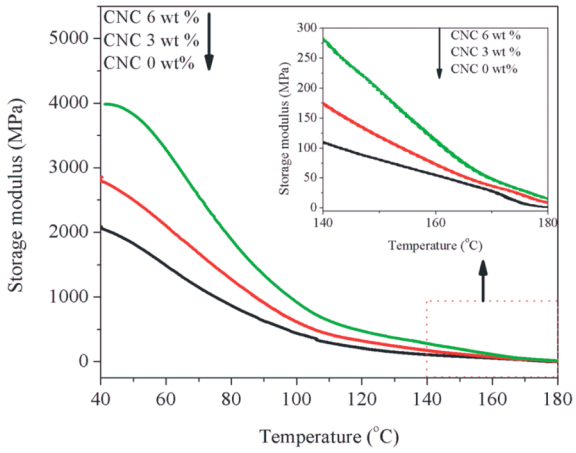

Figure 2. Storage modulus of PVDF/PMMA blend and its composites measured by DMA.

the addition of 3 and 6 wt % CNCs increased the storage modulus at 45 °C from 1960 to 2668 and 3957 MPa, respectively, which is consistent with the results and trend obtained from static tensile testing. The reinforcing effect was maintained at high temperatures (the magnified portion of the curve in Figure 2). For instance, the storage modulus of PVDF/PMMA blend at 150 °C was 80 MPa compared with 119 and 196 MPa for composite with 3 and 6 wt % CNCs, respectively. Such a reinforcing effect can be attributed to the fact that the polymeric matrix was softened at high temperatures, while the rigidity of CNCs was still well maintained.

Hydrophilicity. Figure 3 summarizes the static water contact angle data of different materials. Pure PVDF exhibited a water contact angle value of 89°. With the addition of PMMA, the water contact angle of the composite decreased to 77° and

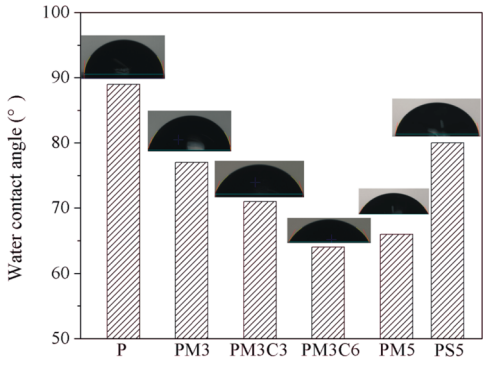

Figure 3. Comparison of static water contact angle of different materials from the study.

66° for the PVDF/PMMA (70/30) blend and the PVDF/PMMA (50/50) blend, respectively. For the PVDF/SAN blend system, even the addition of 50 wt % SAN only reduced the water contact angle to 80°. All these results indicate that the hydrophilic modification of both PMMA and SAN was of low efficiency.

In a sharp contrast, a drastic improvement in the efficiency of hydrophilic modification was achieved when PMMA and CNCs were combined. With the addition of 6 wt % CNCs into the PVDF/PMMA (70/30) matrix, the water contact angle of materials decreased to 64°, and the value was even lower than that of the PVDF/PMMA (50/50) blend (66°). Therefore, it is obvious that CNCs are more effective to improve the hydrophilicity of PVDF than the addition of a second polymer.

Thermal Stability. In addition to reinforcement and the improved hydrophilicity, thermal stability of composites was also considerably improved. TG curves and derivative thermogavimetric (DTG) curves of pure CNCs, PVDF/PMMA blend and its composites are shown in Figure 4. The

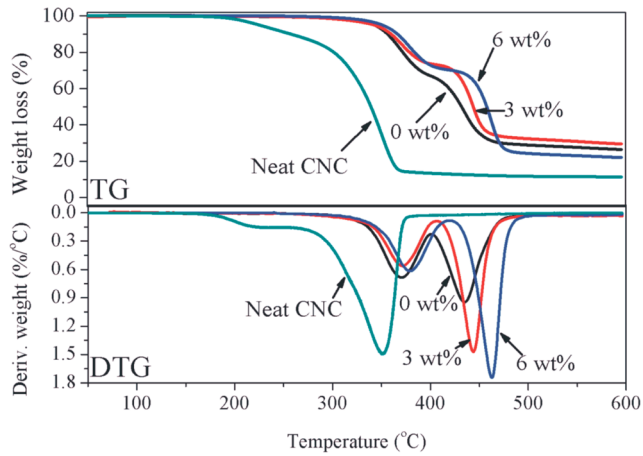

Figure 4. TG and DTG curves of PVDF/PMMA blend and its composites.

detailed results obtained from TG and DTG curves are summarized in Table 2. Pure CNCs exhibited one degradation step within the tested temperature region. The PVDF/PMMA blend showed two degradation steps. The first degradation step, which was at temperatures up to about 400 °C, corresponded to the degradation of PMMA.[28] The second degradation step, which occurred in the temperature range of 400−600 °C, was attributed to the decomposition of PVDF.[28] Similar to the

DOI: 10.1021/sc500792c
ACS Sustainable Chem. Eng. 2015, 3, 574−582

Table 2. TGA and DSC Results of PVDF/PMMA Blend and Its Composites

sample	T_{onset} [a] (°C)	$T_{50\%}$ [a] (°C)	T_{p1} [a] (°C)	T_{p2} [a] (°C)	T_m^p [b] (°C)	T_c^p [b] (°C)	$t_{1/2}$ [b] (°C)	ΔH_m [b] (J·g^{-1})	X_c [b] (%)
PMC0	356.4	432.4	370.6	434.8	159.7	123.0	84.7	29.8	28.5
PMC3	360.4	444.3	371.1	443.7	161.6	129.8	63.3	40.4	43.3
PMC6	366.9	459.3	378.9	462.5	162.0	132.3	68.6	34.1	35.3
CNC	258.0	339.8	350.9						

[a] T_{onset} and $T_{50\%}$: the temperatures corresponding to 10 wt %, and 50 wt % of weight loss. T_{p1} and T_{p2}: the temperatures corresponding to the first and the second peak of the DTG curve. [b] T_m^p: peak melting temperature of PVDF. T_c^p: peak crystallization temperature of PVDF. $t_{1/2}$: the half time of crystallization. ΔH_m: melting enthalpy of PVDF. X_c: crystallinity of PVDF.

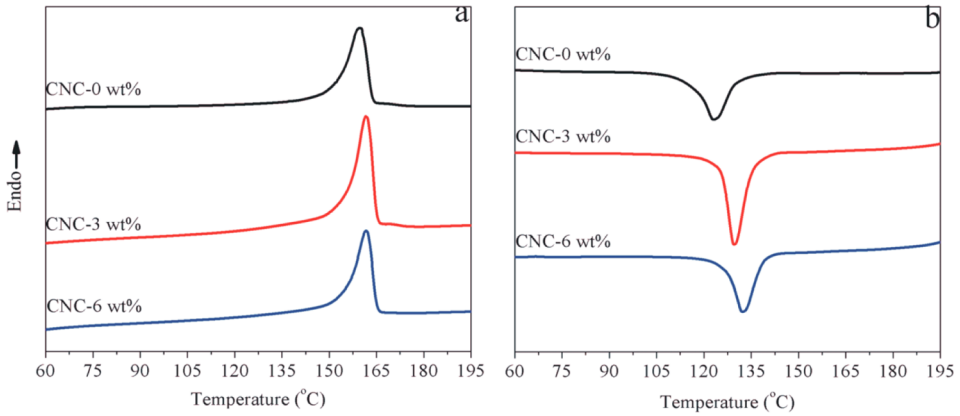

Figure 5. Melting and crystallization behaviors measured by DSC: (a) melting curves; (b) crystallization curves.

degradation behavior of the PVDF/PMMA blend, ternary composites still exhibited two degradation steps. However, an interesting contrast was observed in the DTG curves. The change in the second peak was more obvious than that in the first. With the addition of CNCs, the second peak height considerably increased and the peak temperature (T_{p2}) considerably shifted to high temperature region (e.g., the T_{p2} increased from 434.8 to 462.5 °C with the addition of 6 wt % CNCs). However, the first peak height slightly decreased and less obvious shift of the peak temperature was observed. This contrast indicated that some structural changes existed in composites, and CNCs affected more on the PVDF component than the PMMA component.

The onset decomposition temperature (T_{onset}) of pure CNCs was 258.0 °C, which is lower than that of the pure PVDF/PMMA blend (356.4 °C), indicating the lower thermal stability of CNCs compared with that of PVDF/PMMA blend. However, it is interesting to note that addition of CNCs improved the thermal stability as verified by the improved values of T_{onset} and $T_{50\%}$. For example, T_{onset} and $T_{50\%}$ exhibited an increase of 10.5 and 26.9 °C with the addition of 6 wt % CNCs. The improved thermal stability was unexpected, because CNCs were less thermally stable than PVDF/PMMA blend (further discussion in the Mechanisms for the Improved Performance section).

Melting and Crystallization Behaviors. The measured DSC curves and related parameters are shown in Figure 5 and Table 2, respectively. For melting behaviors (Figure 5a), the peak melting temperature (T_m^p) of the blends was shifted from 159.7 to 162.0 °C with the addition of CNCs from 0 to 6 wt %. The results indicated that addition of CNCs increased the thickness of lamellar crystals of PVDF.[29] Besides the increase in peak melting temperature, the crystallinity of PVDF (X_c) considerably increased (from 28.5% for PVDF/PMMA blend to 43.3% for composite with 3 wt % CNCs). For a semicrystalline polymer such as PVDF, its mechanical strength strongly depends upon its crystallinity. Usually, higher crystallinity is accompanied by higher mechanical strength.[18] Therefore, the enhanced crystallinity induced by CNCs is thought to be responsible for the aforementioned reinforcing effect on mechanical properties. However, it seems that CNCs first led to an increase of crystallinity followed by decreasing from 43.3% to 35.3% when CNC content further increased to 6 wt %. Similar trend regarding crystallinity was also reported in other articles.[29,30] Generally, two factors corresponding to the nucleating and diffusion effects exerted by fillers[31] determine the crystallinity and crystallization behaviors of polymer composites. The nucleating effect is usually observed at low nanofiller content, which favors the crystallization of polymers. The diffusion effect occurs at high nanofiller contents, based on which the motion of polymer chains was hindered and therefore played a negative role in the crystallization of polymers.[32,33] In this work, when CNC content was 3 wt %, the nucleating effect of CNCs took the leading place, which helped enhance the ability of PVDF chains to crystallize and therefore contributed to the large improvement in crystallinity. As the CNCs content further increased to 6 wt %, the diffusion effect became stronger and therefore contributed to the decrease in crystallinity, although the value of crystallinity was higher than that of pure PVDF/PMMA blend.

For nonisothermal crystallization behaviors (Figure 5b), the use of CNCs increased the peak crystallization temperature (T_c^p) of PVDF drastically (e.g., 3 wt % CNCs resulting in an increase of 7 °C.), indicating the nucleating effect of CNCs. A slight increase of 2 °C was observed when 6 wt % CNCs was added. Such a slight increase was attributed to the diffusion effect of CNCs. For crystallization rate, its trend was similar to that of crystallinity. CNCs first contributed to a considerable increase in crystallization rate ($t_{1/2}$ decreased from 84.7 to 63.3 s) followed with a slight decrease as CNC content increased to

DOI: 10.1021/sc500792c
ACS Sustainable Chem. Eng. 2015, 3, 574−582

6 wt % ($t_{1/2}$ increased from 63.3 to 68.6 s). The trend in crystallization rate could also be explained by the competition between nucleating effect and diffusion effect of CNCs.

The trend of $t_{1/2}$ was also verified by isothermal crystallization tests through measuring the storage modulus as a function of time immediately after decreasing to a given isothermal temperature from polymer melt rapidly (Figure 6).

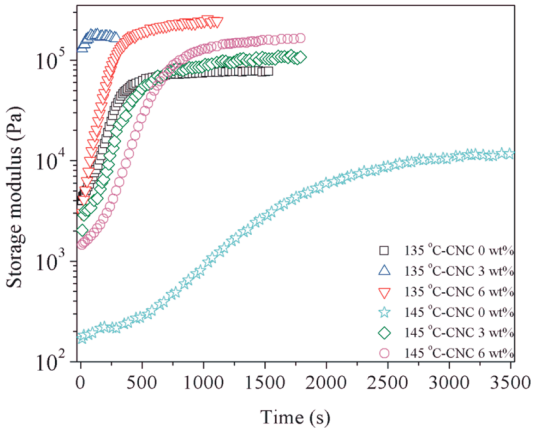

Figure 6. Time evolution of storage modulus for PVDF/PMMA blend and its composites.

Briefly, storage modulus first exhibited a sharp increase, and then reached a plateau, which corresponded to processes of crystal growth and the completed crystallization, respectively.[34] The shorter the time needed to reach the plateau of storage modulus, the higher crystallization rate the material will exhibit. As shown in Figure 6, incorporation of CNCs considerably decreased the time needed to reach the plateau (e.g., comparing the data represented by cycle symbols with those shown by pentagram symbols (composites 6 wt % CNCs at 145 °C). In addition, composites with 6 wt % CNCs required more time to reach the plateau than composite with 3 wt % CNCs. Therefore, the order of isothermal crystallization rate was: composite with 3 wt % CNCs > composite with 6 wt % CNCs >PVDF/PMMA blend, which was consistent with the results of $t_{1/2}$ measured by DSC. Besides the enhanced isothermal crystallization rate, the storage modulus at the plateau was higher for composites than that for PVDF/PMMA blend, which again verified the reinforcing effect of CNCs.

Morphology. SEM images of the cryo-fractured surfaces of different samples are shown in Figure 7. As shown in Figure 7a, no obvious phase separation existed and a uniform pattern was observed, indicating a good compatibility between PVDF and PMMA. In addition, no PVDF spherulites were observed. However, with the addition of 3 wt % of CNCs, PVDF spherulites were formed and fully dispersed within the PVDF/PMMA matrix (Figure 7b). This indicated that CNCs favored the crystallization of PVDF and the formation of PVDF spherulites. As CNC content further increased to 6 wt %, the spherulites exhibited a smaller size and distributed less uniformly (see Figure 7c). This was ascribed to the diffusion effect of CNCs, which reduced the free volume of PVDF and retarded the crystallization of PVDF.[3] All the results of the morphology corresponded well with the aforementioned DSC results.

FTIR Analysis. It is well-known that PVDF has at least four crystalline phases: α, β, γ and δ phases, and the change in the crystalline phase can influence the properties of PVDF.[3] Usually, different crystalline phases exhibited different characteristic peaks fewer than 2000 cm^{-1} in Fourier transform infrared spectroscopy (FTIR).[1,3] In this work, the characteristic peaks less than 2000 cm^{-1} exhibited no obvious changes (Figure 8A), indicating that incorporation of CNCs did not change the types of crystalline phases of PVDF.[1,3] Therefore, it seems that the improved performance could not be attributed

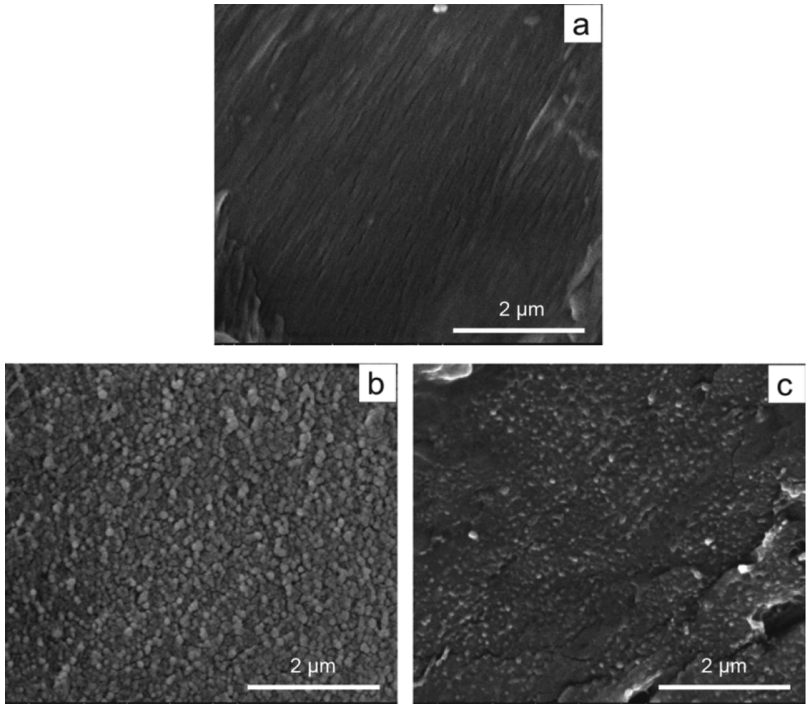

Figure 7. Morphology of blend and composites: (a) PVDF/PMMA blend; (b) composite with 3 wt % CNCs; (c) composite with 6 wt % CNCs.

DOI: 10.1021/sc500792c
ACS Sustainable Chem. Eng. 2015, 3, 574−582

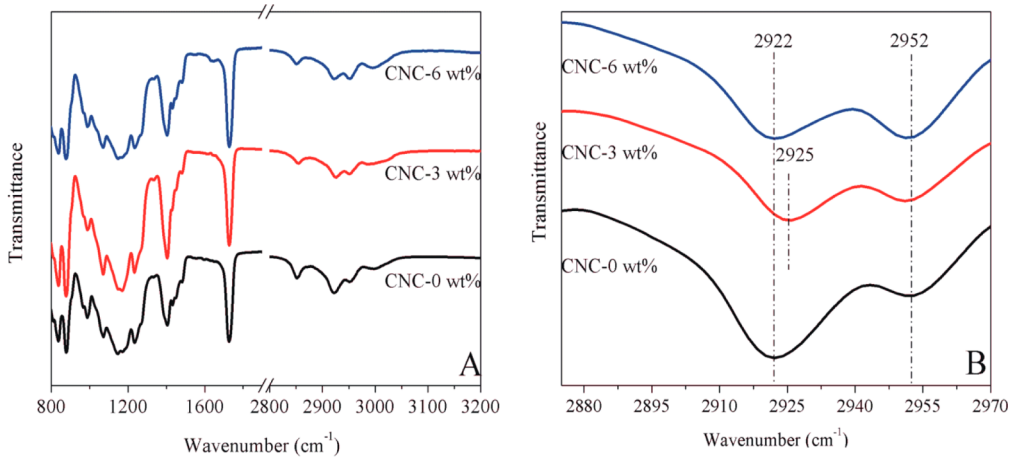

Figure 8. FTIR curves of PVDF/PMMA (70/30) blend and its composites (A) and symmetric vibration of CH_2 group in PVDF and C−O−CH_3 stretching in PMMA (B).

to the change in the crystal type. However, the peak at 2922 cm^{-1} referring to the symmetric vibration of CH_2 group in PVDF[35] in Figure 8B shifted to 2925 cm^{-1} with the addition of 3 wt % CNCs. However, in a sharp contrast, no shift was observed regarding the peak at 1147 cm^{-1} assigned to the symmetrical stretching of the CF_2 group (see Figure 8B).[36] This confirms that PVDF chains selectively interacted with CNCs from its hydrogen atoms side rather than its fluorine atoms side. Such an interaction is helpful to induce the nucleating effect observed in DSC tests. Moreover, the ratio between the height of the peak at 2922 cm^{-1} referring to the symmetric vibration of the CH_2 group in PVDF and the height of peak at 2952 cm^{-1} corresponding to the C−O−CH_3 stretching in PMMA[36] decreased as CNCs content increased. This feature indicated that the addition of CNCs interacted more with PVDF than PMMA.

Mechanisms for the Improved Performance. Based on the above results, a scheme of the structural change caused by CNCs is proposed and displayed in Figure 9. For neat the PVDF/PMMA blend, some PVDF chains were arranged into a lattice to form the crystal region, whereas mobility of the other PVDF chains (amorphous phase) was restricted by PMMA chains (Figure 9A), due to the strong affinity between PVDF and PMMA.[1] With the addition of 3 wt % CNCs, two effects were introduced (Figure 9B). First, CNCs induced a certain interaction with the CH_2 group in PVDF (as verified by FTIR), which helped PVDF chains being absorbed to the surface of CNCs and therefore induced a nucleating effect on crystallization. Second, CNCs also had an affinity toward PMMA.[16] Thus, some PVDF chains (amorphous phase) restricted by PMMA were freed, based on which the liberated PVDF chains rearranged into the lattice, leading to the formation of polymeric spherulites (see Figure 9B) and increase in both the crystallinity and crystallization rate of PVDF. For semicrystalline polymers like PVDF, its strength and modulus depend upon its crystallinity.[18] Thus, the increased crystallinity was the main reinforcement mechanism. When CNC content further increased to 6 wt % (Figure 9C), the nucleating effect of CNCs became saturated. Instead, the diffusion effect of CNCs even hindered the rearrangement of PVDF chains into lattice,[3,33] causing decreases in crystallinity and crystallization rate (still higher than those of pure blend). As a result, the tensile strength even slightly decreased compared with that of the composite with 3 wt % CNCs. In this case, the reinforcement was partly due to the rigid nature of CNCs.

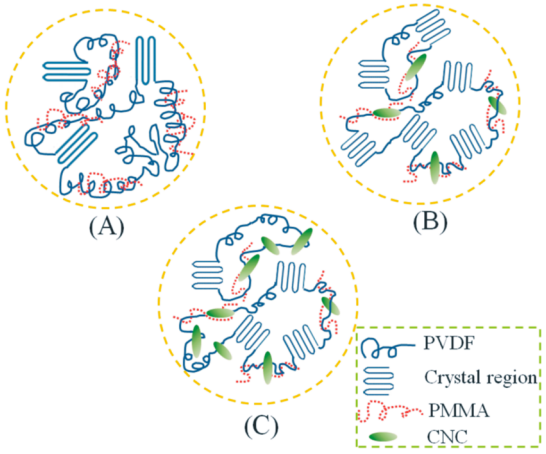

Figure 9. Schematic representation of the mechanism for the improved performance: (A) PVDF/PMMA blend; (B) composite with 3 wt % CNCs; (C) composite with 6 wt % CNCs.

For the mechanism of the improved thermal stability, it can be explained by the following two factors. First, the enhanced crystallinity made PVDF lattices to become more thermally stable.[37] Second, the interaction between CNCs and the CH_2 group in PVDF made CNCs to be surrounded by PVDF lattice (CNCs worked as nuclei), and therefore helped prevent CNCs from being thermally degraded under the thermal degrading conditions. Therefore, a higher thermal stability was obtained, even though CNCs themselves had a relatively poor nature of thermal stability in comparison with that of the pure PVDF/PMMA blend. For the mechanism of the improved hydrophilicity, the hydrophilic nature of CNCs is responsible for the improvement.

CONCLUSIONS

Previous studies[1,5−7] focused on improving the hydrophilicity of PVDF using hydrophilic polymers. In this work, PMMA and CNCs were combined to modify the hydrophilicity of PVDF. In comparison with polymers such as PMMA and SAN, the combination of PMMA and a small amount of CNCs not only

DOI: 10.1021/sc500792c
ACS Sustainable Chem. Eng. 2015, 3, 574−582

exhibited a higher efficiency of hydrophilic modification but also achieved an impressive reinforcement. The improvements were mainly attributed to the hydrophilic nature of CNCs and the effect of CNCs on the crystallization behavior of PVDF. The addition of CNCs favored the crystallization of PVDF via exerting nucleating effect on PVDF/PMMA matrix. As a result, the crystallinity of PVDF was drastically enhanced and the crystallization rate was also accelerated. The increased crystallinity helped increase the tensile strength, tensile and storage modulus and the onset thermal decomposition temperature. CNCs did not change the types of crystalline phase of PVDF, and CNCs interacted more with PVDF than PMMA in the composite. In comparison with previous literature reports,[1,5−7] our present study demonstrates a facile pathway to fabricate PVDF-based nanocomposites with enhanced performance.

■ ASSOCIATED CONTENT

Supporting Information

FTIR and TGA curves of PVDF/PMMA/CNCs composite with 3 wt% CNCs before and after ethanol extraction. This material is available free of charge via the Internet at http://pubs.acs.org.

■ AUTHOR INFORMATION

Corresponding Authors

*Q. Wu. E-mail: wuqing@lsu.edu.
*T. Lei. E-mail: leitingzhou@163.com.

Notes

The authors declare no competing financial interest.

■ ACKNOWLEDGMENTS

We express our sincere gratitude for the support from the Economic Development Assistantship Program at Louisianan State University, and from the Key Biomass Energy Laboratory of Henan Province, China.

■ REFERENCES

(1) Ma, W.; Zhang, J.; Wang, X.; Wang, S. Effect of PMMA on crystallization behavior and hydrophilicity of poly(vinylidene fluoride)/poly(methyl methacrylate) blend prepared in semi-dilute solutions. *Appl. Surf. Sci.* **2007**, *253*, 8377−8388.

(2) Shi, H.; Liu, F.; Xue, L.; Lu, H.; Zhou, Q. Enhancing antibacterial performances of PVDF hollow fibers by embedding Ag-loaded zeolites on the membrane outer layer via co-extruding technique. *Compos. Sci. Technol.* **2014**, *96*, 1−6.

(3) Zhao, X.; Zhang, W.; Chen, S.; Zhang, J.; Wang, X. Hydrophilicity and crystallization behavior of PVDF/PMMA/TiO_2 (SiO_2) composites prepared by in situ polymerization. *J. Polym. Res.* **2012**, *19*, 1−9.

(4) Girard, E.; Marty, J. D.; Ameduri, B.; Destarac, M. Direct synthesis of vinylidene fluoride-based amphiphilic diblock copolymers by RAFT/MADIX polymerization. *ACS Marco Lett.* **2012**, *1*, 270−274.

(5) Nunes, S. P., Peinemann, K. V. *Membrane Technology in the Chemical Industry*; Wiley-VCH: Weinhein, Germany, 2001; p 12.

(6) Ma, W.; Zhang, J.; Chen, S.; Wang, X. Crystallization behavior and hydrophilicity of poly(vinylidene fluoride) (PVDF)/poly(styrene-co-acrylonitrile) (SAN) blends. *Colloid Polym. Sci.* **2008**, *286*, 1193−1202.

(7) Chen, J.; Wang, S.; Chen, S.; Zhang, J.; Wang, X. Crystallization behavior and hydrophilicity of poly(vinylidene fluoride)/poly(methyl methacrylate)/poly(vinyl pyrrolidone) ternary blends. *Polym. Int.* **2012**, *61*, 477−484.

(8) Yin, X.; Cheng, H.; Wang, X.; Yao, Y. Morphology and properties of hollow-fiber membrane made by PAN mixing with small amount of PVDF. *J. Membr. Sci.* **1998**, *146*, 179−184.

(9) Li, N.; Xiao, C.; An, S.; Hu, X. Preparation and properties of PVDF/PVA hollow fiber membranes. *Desalination* **2010**, *250*, 530−537.

(10) Salam, A.; Lucia, L.; Jameel, H. A novel cellulose nanocrystals-based approach to improve the mechanical properties of recycled paper. *ACS Sustainable Chem. Eng.* **2013**, *1*, 1584−1592.

(11) Huang, J.; Li, C.; Gray, D. Cellulose nanocrystals incorporating fluorescent methylcoumarin groups. *ACS Sustainable Chem. Eng.* **2013**, *1*, 1160−1164.

(12) Hosoda, N.; Tsujimoto, T.; Uyama, H. Green composite of poly(3-hydroxybutyrate-co-3-hydroxyhexanoate) reinforced with porous cellulose. *ACS Sustainable Chem. Eng.* **2014**, *2*, 248−253.

(13) Xu, Q.; Kong, Q.; Liu, Z.; Wang, X.; Liu, R.; Zhang, J.; Yue, L.; Duan, Y.; Cui, G. Cellulose/Polysulfonamide Composite Membrane as a High Performance Lithium-Ion Battery Separator. *ACS Sustainable Chem. Eng.* **2014**, *2*, 194−199.

(14) Mu, C.; Su, Y.; Sun, M.; Chen, W.; Jiang, Z. Remarkable improvement of the performance of poly(vinylidene fluoride) microfiltration membranes by the additive of cellulose acetate. *J. Membr. Sci.* **2010**, *350*, 293−300.

(15) Zhou, C.; Chu, R.; Wu, R.; Wu, Q. Electrospun polyethylene oxide/cellulose nanocrystal composite nanofibrous mats with homogeneous and heterogeneous microstructures. *Biomacromolecules* **2011**, *12*, 2617−2625.

(16) Liu, H.; Liu, D.; Yao, F.; Wu, Q. Fabrication and properties of transparent polymethylmethacrylate/cellulose nanocrystals composites. *Bioresour. Technol.* **2010**, *101*, 5685−5692.

(17) Hu, X.; Xu, C.; Gao, J.; Yang, G.; Geng, C.; Chen, F.; Fu, Q. Toward environment-friendly composites of poly(propylene carbonate) reinforced with cellulose nanocrystals. *Compos. Sci. Technol.* **2013**, *78*, 63−68.

(18) Pei, A.; Zhou, Q.; Berglund, L. A. Functionalized cellulose nanocrystals as biobased nucleation agents in poly(L-lactide)-(PLLA)—Crystallization and mechanical property effects. *Compos. Sci. Technol.* **2010**, *70*, 815−821.

(19) Rueda, L.; Saralegui, A.; Fernández d'Arlas, B.; Zhou, Q.; Berglund, L. A.; Corcuera, M. A.; Mondragon, I.; Eceiza, A. Cellulose nanocrystals/polyurethane nanocomposites. Study from the viewpoint of microphase separated structure. *Carbohydr. Polym.* **2013**, *92*, 751−757.

(20) Zhang, Z.; Song, K.; Wu, Q.; Li, Y. Non-isothermal crystallization of poly(vinylidene fluoride)/poly(methyl methacrylate)/cellulose nanocrystal nanocomposites. *Int. J. Polym. Anal. Charact.* **2014**, *4*, 332−341.

(21) Mathew, A.; Oksman, K.; Sain, M. The effect of morphology and chemical characteristics of cellulose reinforcements on the crystallinity of polylactic acid. *J. Appl. Polym. Sci.* **2006**, *101*, 300−310.

(22) Yue, Y.; Zhou, C.; French, A. D.; Guan bn b, X.; Han, G.; Wang, Q.; Wu, Q. Comparative properties of cellulose nano-crystals from native and mercerized cotton fibers. *Cellulose* **2012**, *19*, 1173−1187.

(23) Nakagawa, K.; Ishida, Y. Annealing effects in poly (vinylidene fluoride) as revealed by specific volume measurements, differential scanning calorimetry, and electron microscopy. *J. Polym. Sci., Part B: Polym. Phys.* **1973**, *11*, 2153−2171.

(24) Zhang, Z.; Zhao, X.; Zhang, J.; Chen, S. Effect of nano-particles-induced phase inversion on largely improved impact toughness of PVC/α-methylstyrene−acrylonitrile copolymer (α-MSAN)/CPE-matrix composites. *Compos. Sci. Technol.* **2013**, *86*, 122−128.

(25) Zhang, Z.; Wang, S.; Zhang, J. Large stabilizing effect of titanium dioxide on photodegradation of PVC/α-methylstyrene-acrylonitrile copolymer/impact modifier-matrix composites. *Polym. Compos.* **2014**, *35*, 2365−2375.

(26) Jonoobi, M.; Harun, J.; Mathew, A. P.; Oksman, K. Mechanical properties of cellulose nanofiber (CNF) reinforced polylactic acid (PLA) prepared by twin screw extrusion. *Compos. Sci. Technol.* **2010**, *70*, 1742−1747.

DOI: 10.1021/sc500792c
ACS Sustainable Chem. Eng. 2015, 3, 574−582

(27) Xu, X.; Liu, F.; Jiang, L.; Zhu, J. Y.; Haagenson, D.; Wiesenborn, D. P. Cellulose nanocrystals vs. cellulose nanofibrils: A comparative study on their microstructures and effects as polymer reinforcing agents. *ACS Appl. Mater. Interfaces* **2013**, *5*, 2999−3009.
(28) Pramoda, K. P.; Linh, N. T. T.; Tang, P. S.; Tjiu, W. C.; Goh, S. H.; He, C. B. Thermo-mechanical properties of poly(vinylidene fluoride) modified graphite/poly(methyl methacrylate) nano composites. *Compos. Sci. Technol.* **2010**, *70*, 578−583.
(29) Azizi Samir, M. A. S.; Alloin, F.; Sanchez, J. Y.; Dufresne, A. Cellulose nanocrystals reinforced poly(oxyethylene). *Polymer* **2004**, *45*, 4149−4157.
(30) Dufresne, A. Polysaccharide nano crystal reinforced nanocomposites. *Can. J. Chem.* **2008**, *86*, 484−494.
(31) Jimenez, G.; Ogata, N.; Kawai, H.; Ogihara, T. Structure and thermal/mechanical properties of poly(ϵ-caprolactone)-clay blend. *J. Appl. Polym. Sci.* **1997**, *64*, 2211−2220.
(32) Siqueira, G.; Bras, J.; Follain, N.; Belbekhouche, S.; Marais, S.; Dufresne, A. Thermal and mechanical properties of bio-nanocomposites reinforced by *Luffa cylindrica* cellulose nanocrystals. *Carbohydr. Polym.* **2013**, *91*, 711−717.
(33) Wang, S.; Zhang, J. Non-isothermal crystallization kinetics of high density polyethylene/titanium dioxide composites via melt blending. *J. Therm. Anal. Calorim.* **2014**, *115*, 63−71.
(34) Chae, D. W.; Hong, S. M. Rheology, crystallization behavior under shear, and resultant morphology of PVDF/multiwalled carbon nanotube composites. *Macromol. Res.* **2011**, *19*, 326−331.
(35) Sharma, M.; Sharma, K.; Bose, S. Segmental relaxations and crystallization-induced phase separation in PVDF/PMMA blends in the presence of surface-functionalized multiwall carbon nanotubes. *J. Phys. Chem. B* **2013**, *117*, 8589−8602.
(36) Mohamadi, S.; Sharifi-Sanjani, N.; Foyouhi, A. Evaluation of graphene nanosheets influence on the physical properties of PVDF/PMMA blend. *J. Polym. Res.* **2012**, *20*, 1−10.
(37) Hung, C. Y.; Wang, C. C.; Chen, C. Y. Enhanced the thermal stability and crystallinity of polylactic acid (PLA) by incorporated reactive PS-b-PMMA-b-PGMA and PS-b-PGMA block copolymers as chain extenders. *Polymer* **2013**, *54*, 1860−1866.

DOI: 10.1021/sc500792c
ACS Sustainable Chem. Eng. 2015, 3, 574−582